

微量稀土镧钕对 Bi5Sb8Sn 力学性能影响

李 帅, 闫焉服, 冯丽芳, 赵永猛

(河南科技大学 材料科学与工程学院, 洛阳 471023)

摘 要: 通过在 Bi5Sb8Sn 基体钎料上添加微量稀土镧钕形成 Bi5Sb8SnRE 新型钎料合金, 研究了稀土镧钕对钎料合金力学性能的影响, 同时对显微组织进行了分析。结果表明, 稀土镧钕含量为 0.2% 时, Bi5Sb8SnRE 合金抗拉强度和抗剪强度达到最大值, 分别为 58.30 MPa 和 15.50 MPa, 合金抗拉强度和钎焊接头的抗剪强度较基体钎料 Bi5Sb8Sn 分别提高了 44.2% 和 57.0%。显微组织分析表明, 微量稀土镧钕的添加能显著细化该钎料的合金组织, 改善合金的组织分布, 提高钎料的力学性能; 但当稀土含量超过 0.2% 时, 稀土化合物的数量增多, 钎料的力学性能下降。

关键词: 新型钎料合金; 稀土镧钕; 抗拉强度; 抗剪强度

中图分类号: TG 425 **文献标识码:** A **文章编号:** 0253-360X(2014)07-0009-04

0 序 言

由于结构形式和使用要求等方面差异, 有些电子产品或某些器件必须用高温软钎料来焊接, 尤其在电子组装中分步钎焊时, 先组装的部分需要采用较高熔点的钎料。常用的高温软钎料主要有高铅钎料、金基钎料、铋基钎料^[1-2]。高铅钎料成本低, 钎焊性能优越, 综合性能好, 但铅有毒, 污染环境, 危害人类健康; 常用金基钎料的有 Au-20Sn(熔点 280 ℃), Au-30Si(熔点 370 ℃) 和 Au-26Ge(熔点 350 ℃) 等共晶体系钎料^[3], 但金价格昂贵且易形成脆的 AuSn₄ 金属间化合物, 使其应用受到很大限制; Bi-Ag 合金是一种可行的电子芯片粘接无铅钎料, 但其在铜基板上润湿性较好而在镀镍基板上较差, 且 Bi-2.5Ag/Ni, Bi-41Ag/Ni 在钎焊接头界面处易生成有灰色胞状 NiBi₃, 导致焊点可靠性不良^[4-6], 因此研究开发无铅高温软钎料产品显得尤为重要。

Bi5Sb 钎料合金熔点在 250 ~ 350 ℃ 之间, 价格低, 力学性能优良, 是一种具有推广应用前景的二元无铅高温软钎料, 但 Bi5Sb 合金脆性大, 加工性差且润湿性不良。作者所在团队的前期研究表明^[7], 在 Bi5Sb 中添加不同含量的锡, Bi5Sb8Sn 熔点合适, 钎焊工艺性能明显改善, 但力学性能有待进一步提高。文中通过在 Bi5Sb8Sn 合金中加入微量混合稀土镧钕形成新型合金, 来改善钎料力学性能。

1 试验方法

1.1 合金的制备

试验所用的原材料为分析纯 Bi、纯 Sb、纯 Cu、纯 Sn, 混合稀土, 其纯度均为 99.95% (质量分数)。将 Bi、Sb、Cu、Sn 或稀土按表 1 所示比例用电子天平进行称取, 误差为 ±1%。在真空度为 5×10^{-3} Pa 的非自耗真空电炉 ZHW-600A 中熔炼, 熔炼过程中为保证合金组织的均匀度, 将合金翻转反复熔炼三次, 浇铸成棒料, 一部分用来加工成拉伸试棒, 剩下的分别轧成 0.1 mm 厚的薄带, 待用。

表 1 试验选用的 BiSbSnRE 钎料合金系列
Table 1 Series of examined BiSbSnRE solder alloy

初始合金	序号	稀土含量 w (质量分数, %)	序号	稀土含量 w (质量分数, %)
Bi-5.0Sb-8.0Sn	1	0	3	0.2
	2	0.1	4	0.3

注: Bi、Sb、Sn 按添加元素后余量的 95.0:5.0:8.0 质量比进行配制

1.2 抗拉强度的测定

根据国家标准 GB11363—89, 拉伸试样尺寸如图 1 所示。为消除残余应力影响, 对拉伸试样进行回火处理, 回火工艺为 100 ℃/2 h。拉伸试验在 AG-1250KN 万能实验机上进行, 加载速率为 1 mm/min, 测试温度为 25 ℃。每种成分做 3 个试样, 求其平均值作为该成分钎焊试样的抗拉强度。

1.3 抗剪强度的测定

剪切试样如图 2 所示, 试样基板为黄铜(纯度为

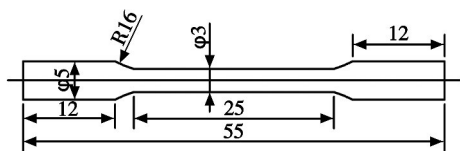


图 1 拉伸试验试样 (mm)

Fig. 1 Specimen for tensile test

99.95%) ,焊缝厚度为 0.1 mm. 为保证焊缝的厚度,在搭接接头钎料中间加入两段 $\phi 0.1$ mm 的铜丝. 为消除残余应力,试样在剪切前进行 100 $^{\circ}\text{C}$,保温 2 h 回火处理. 抗剪强度试验在 AG-1250KN 万能实验机上进行,加载速率为 1 mm/min,测试温度为 25 $^{\circ}\text{C}$. 每种成分作 3 个试样,求其平均值作为该成分钎焊接头的抗剪强度.

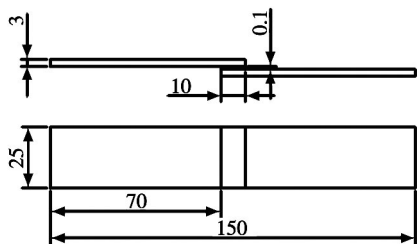


图 2 剪切试验试样 (mm)

Fig. 2 Specimen for shear test

2 结果与讨论

2.1 稀土镧钎对钎料 Bi5Sb8Sn 抗拉强度影响

微量镧钎对 Bi5Sb8Sn 钎料抗拉强度的影响如图 3 所示,可以看出:当稀土含量小于 0.2% 时,随着稀土含量增加,新型钎料的抗拉强度呈增大趋势;当稀土含量大于 0.2% ,钎料合金抗拉强度随着稀土含量增加呈下降趋势;当稀土含量为 0.2% 时, Bi5Sb8Sn0.2RE 抗拉强度为 58.30 MPa ,较基体钎料

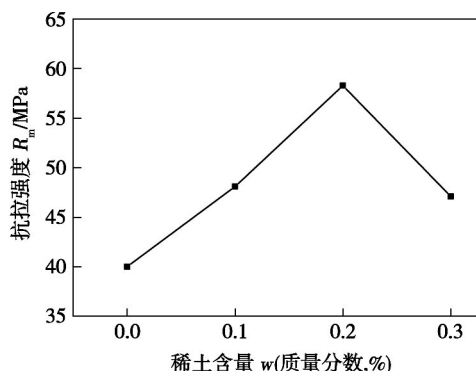
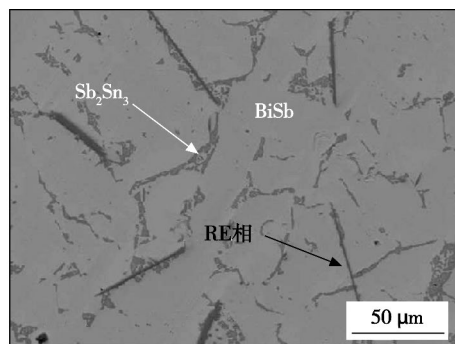


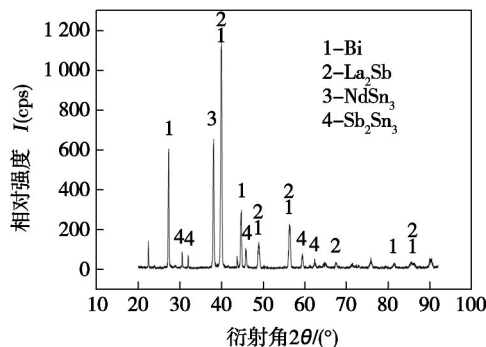
图 3 (Bi5Sb8Sn) RE 钎料合金抗拉强度

提高了 44.2% .

图 4 为 Bi5Sb8Sn0.3RE 钎料 SEM 图像和 X 射线衍射分析,可知形成的化合物主要有金属间化合物大块白色的 BiSb 相、浅灰色的 Sb_2Sn_3 及长条状的稀土相 La_2Sb 和 NdSn_3 组成. 一般地,钎料合金的力学性能与钎料组织的形态和含量有关^[8-9]. 图 5 为钎料合金 Bi5Sb8SnRE 微观组织. 可以看出:基体合金 Bi5Sb8Sn 主要由 Sb_2Sn_3 和 BiSb 固溶体组成,如图 5a 所示. 在基体钎料 Bi5Sb8Sn 中添加 0.2% 的稀土镧钎,稀土相 La_2Sb 和 NdSn_3 取代了基体钎料黑色针状 SnSb 相,且稀土相长度增加,呈现断续状. 另外,稀土添加还可使网状的金属间化合物 Sb_2Sn_3 相细化,即当稀土含量小于 0.2% 时,稀土对基体钎料具有细化组织作用. 细化的组织和新生成的针状 RE 相均匀分布在钎料基体内部,具有弥散强化作用. 同时混合稀土镧钎在钎料合金中是表面活性元素,易聚集在相界,降低界面能和相界能,提高界面结合力,从而提高钎料的力学性能. 因此,当稀土含量小于 0.2% 时,随着稀土含量增加, Bi5Sb8SnRE 钎料的抗拉强度呈增大趋势.



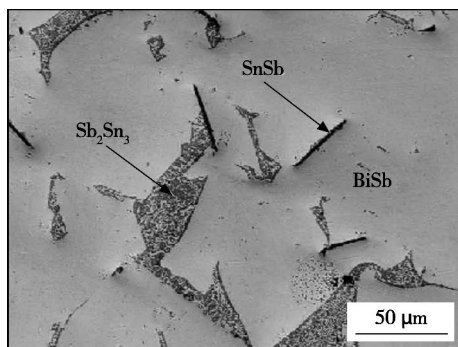
(a) 扫描电镜图



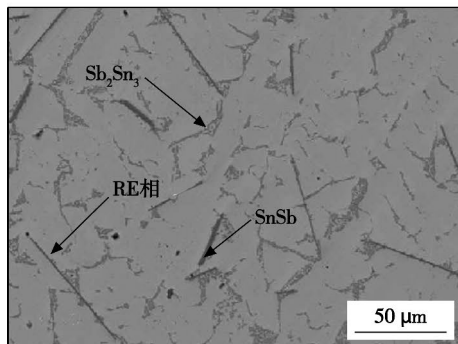
(b) X射线衍射分析

图 4 Bi5Sb8Sn0.3% RE 钎料 SEM 和 X 射线衍射分析
Fig. 4 SEM (a) and XRD (b) of (Bi5Sb8Sn) 0.3% RE solder alloy

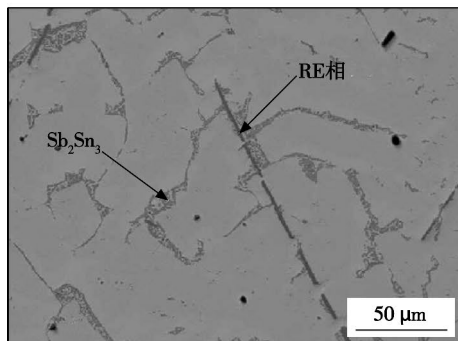
当稀土含量大于 0.2% 时,随着稀土含量增加,



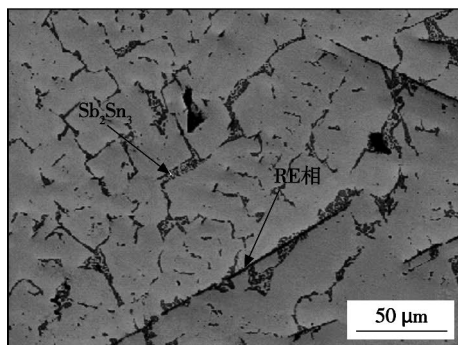
(a) Bi5Sb8Sn



(b) Bi5Sb8Sn0.1% RE



(c) Bi5Sb8Sn0.2% RE



(d) Bi5Sb8Sn0.3% RE

网状的金属间化合物 Sb_2Sn_3 和相和针状的稀土相

图5 钎料合金 Bi5Sb8SnRE 微观组织

Fig. 5 Microstructure of Bi5Sb8SnRE solder alloy

表2 (BiSbSn) RE/Cu 金属间化合物的厚度变化

Table 2 Thickness of intermetallic components of (BiSbSn) RE /Cu solder alloy

初始合金	稀土含量 w (质量分数, %)	金属间化合物厚度 $d/\mu m$	稀土含量 w (质量分数, %)	金属间化合物厚度 $d/\mu m$
Bi-5.0Sb-8.0Sn	0	0.10	0.20	0.30
	15.10	11.24	10.70	12.31

La_2Sb 和 $NdSn_3$ 变多(图5d),即添加过多稀土,导致脆性相 Sb_2Sn_3 增多、稀土相由短棒状向长棒状过渡,因此稀土含量大于 0.2% 时,随着稀土含量增加,钎料合金的抗拉强度呈下降趋势^[10].

2.2 稀土镧钨对钎料 Bi5Sb8Sn 钎焊接头抗剪强度的影响

在相同试验条件下,微量稀土镧钨对 Bi5Sb8Sn 钎焊接头抗剪强度的影响如图6所示,可以看出:当稀土含量小于 0.2% 时,钎料钎焊接头的抗剪强度增大;稀土含量为 0.2% 时,钎焊接头抗剪强度最大为 15.50 MPa,较基体钎提高了 57.0%.

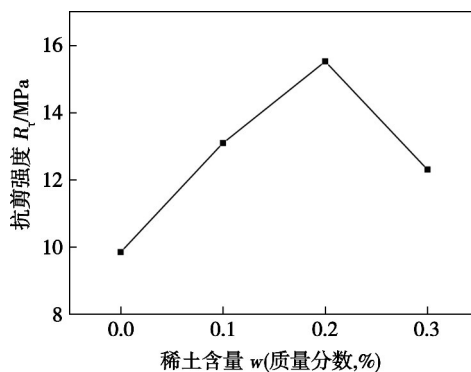
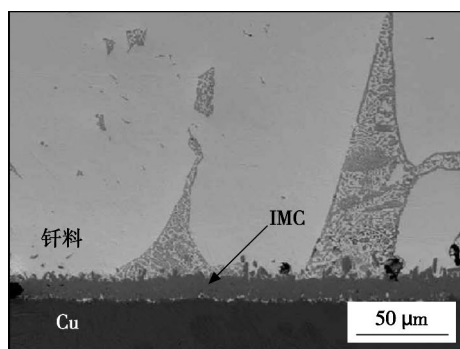


图6 Bi5Sb8SnRE 钎料合金抗剪强度

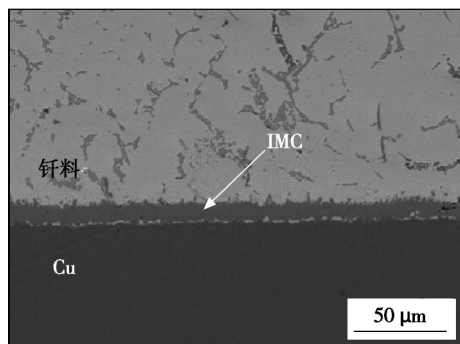
Fig. 6 Shear strength of Bi5Sb8SnRE solder alloy

图7为 Bi5Sb8SnRE 钎料合金在铜基板上的界面区微观组织,其中白色组织为 BiSb 固溶体,灰色网状组织为 Sb_2Sn_3 . 对比图7a和图7b,可以看出:在 Bi5Sb8Sn 无铅钎料中添加少量稀土镧钨, Sb_2Sn_3 变得细密和均匀,相对均匀的分布在钎料基体内部,并呈现断续状分布.正是由于微量稀土镧钨可以细化 Bi5Sb8Sn 微观组织,使 Bi5Sb8SnRE 钎焊接头的剪切强度逐渐增加.图7d为 Bi5Sb8Sn0.3RE 在铜基板上的界面区微观组织,可以看出:当稀土含量大于 0.2% 时,金属间化合物含量过多,且组织有粗化趋势,导致钎焊接头的抗剪强度呈下降趋势.

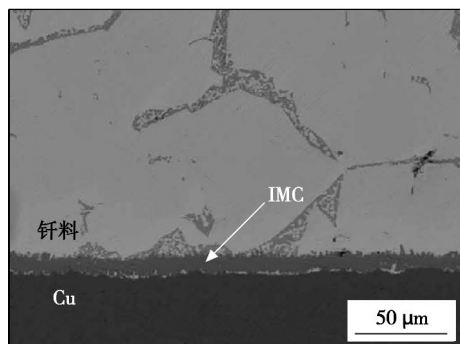
钎焊接头抗剪强度的大小还与铜基板与钎料相互作用生成的界面金属间化合物有关.过厚的金属间化合物层会导致钎焊接头断裂韧性和抗疲劳能力下降,从而导致接头抗剪强度降低^[11].表2为金



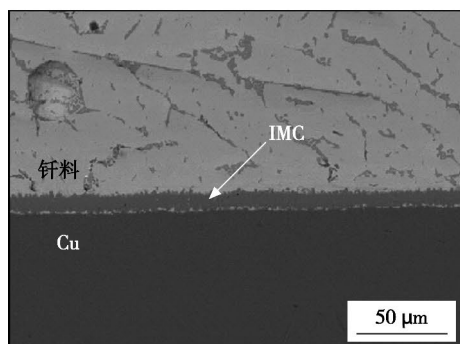
(a) Bi5Sb8Sn



(b) (Bi5Sb8Sn)0.1% RE



(c) (Bi5Sb8Sn)0.2% RE



(d) (Bi5Sb8Sn)0.3% RE

图 7 (BiSbSn) RE 合金在 Cu 基板上的界面区微观组织
Fig. 7 Microstructure of interface of (BiSbSn) RE/Cu solder alloy

属间化合物的厚度变化情况,可以看出:微量稀土加入可以细化组织、抑制金属间化合物生长,这是因为金属间化合物晶界会吸附微量稀土,阻止界面金属间化合物生长,使生成的金属间化合物较薄,有利于钎料钎焊接头剪切性能的提高。但稀土含量大于

0.2%时,随着稀土钨钼含量增加,组织粗化,从而导致剪切强度下降。

3 结 论

(1) 在 Bi5Sb8Sn 系无铅钎料中添加少量稀土钨钼后,钎料内部组织变得更为细密和均匀,稀土相增多,由短棒状向长棒状过渡,并呈现断续状分布。

(2) 当稀土钨钼含量为 0.2% 时, Bi5Sb8SnRE 钎料抗拉强度及钎焊接头的抗剪强度均达到最大值,分别为 58.30 MPa 和 15.50 MPa,较基体钎料分别提高了 44.2% 和 57.0% 左右。

参考文献:

- [1] Yoshikazu T, Ikuo O, Ryosuke K. Development of Bi-base high-temperature Pb-free solders with second-phase dispersion: thermodynamic calculation [J]. *Journal of Electronic Materials*, 2006, 35(11): 1926-1932.
- [2] 房卫萍, 史耀武, 夏志东, 等. 电子组装用高温无铅钎料的研究进展 [J]. *电子元件与材料*, 2009, 28(3): 71-74.
Fang Weiping, Shi Yaowu, Xia Zhidong, et al. Research development of high temperature lead-free solders for electronic assembly [J]. *Electronic Components And Materials*, 2009, 28(3): 71-74.
- [3] Kitagawa H, Noguchi H, Kiyabu T. Thermoelectric properties of Bi-Sb semiconducting alloys prepared by quenching and annealing [J]. *Journal of Physics and Chemistry of Solids*, 2004, 65(7): 1223-1227.
- [4] Song J M, Chuang H Y, Wu Z M. Interfacial reaction Bi-Ag high-temperature solders and metallic substrates [J]. *Journal of Electronic Materials*, 2006, 35(5): 1041-1049.
- [5] John N L, Nancy F D, Martin W W. Experimental Investigation of Ge-Doped Bi-11Ag as a new Pb-Free solder alloy for power die attachment [J]. *Journal of Electronic Materials*, 2002, 31(11): 1244-1249.
- [6] 盛阳阳, 闫焉服, 唐 坤, 等. 锡含量对 Bi5Sb 钎料铺展性能及抗拉性能的影响 [J]. *焊接学报*, 2011, 32(6): 85-87.
Sheng Yangyang, Yan Yanfu, Tang Kun, et al. Effect of content of Sn on spreading properties and tensile properties of Bi5Sb solder alloy [J]. *Transactions of the China Welding Institution*, 2011, 32(6): 85-87.
- [7] Manasuevic D, Minic D, Zivkovic D, et al. Experimental study and thermodynamic calculation of Bi-Cu-Sb system phase equilibria [J]. *Intermetallics*, 2008, 16(1): 107-112.
- [8] Zhai Wei, Hong Zhenyu, Wei Bingbo. Ternary eutectic growth of Ag-Cu-Sb alloy within ultrasonic field [J]. *Science in China Series G: Physics, Mechanics & Astronomy*, 2007, 50(4): 500-508.
- [9] 于 洋, 史耀武, 夏志东. BGA 焊点剪切性能的评价 [J]. *稀有金属材料与工程*, 2009, 38(3): 469-472.
Yu Yang, Shi Yaowu, Xia Zhidong. Valuation on the shear properties of BGA solder joint [J]. *Rare Metal Materials And Engineering*, 2009, 38(3): 469-472.

作者简介: 李 帅,男,1986 年出生,硕士研究生。主要从事先进材料连接方面的研究。Email: lyetlishuai@163.com

通讯作者: 闫焉服,男,教授,博士后。Email: yanyanfu1970@sina.com

MAIN TOPICS ,ABSTRACTS & KEY WORDS

Rapid prototyping process based on cold metal transfer arc welding technology

LIU Yibo¹ , SUN Qingjie^{1,3} , JIANG Yunlu² , WU Laijun¹ , SANG Haibo¹ , FENG Jicai¹ (1. Shandong Provincial Key Laboratory of Special Welding Technology , Harbin Institute of Technology at Weihai , Weihai 264209 , China; 2. Institute of Metal Research , Chinese Academy of Science , Shenyang 110016 , China; 3. Mechanical Engineering Mobile Postdoctoral Center , Harbin Institute of Technology , Harbin 150001 , China) . pp 1 - 4

Abstract: In order to develop the rapid prototyping technology , cold metal transfer arc welding process was adopted and the corresponding robot rapid shaping system was set up. The effect of welding current , welding velocity as well as the welding process on the aspect ratio of the single pass weld seam (λ) was studied. Besides that , the effect of the welding current , elevating height and welding process on the shaping of multilayer cylinder specimen were further investigated , the optimal shaping parameter was obtained and the tensile property of the specimen was tested. The results show that , the larger aspect ratio of weld seam is benefit to obtain the rapid shaping specimen with the flat surface and better accuracy. Suitable welding parameter and weld process can control the dimensional accuracy of shaping and obtain specimens with high performance.

Key words: rapid prototyping; cold metal transfer; aluminum alloy; mechanical properties

Ultrasonic brazing of SiC_p/Almatrix composites and Fe36Ni alloy

WEI Jinghui , GAO Xingqiang , YAN Jiuchun , DENG Binghui (State Key Laboratory of Advanced Welding and Joining , Harbin Institute of Technology , Harbin 150001 , China) . pp 5 - 8

Abstract: Fe36Ni alloy was joined to two kinds of SiC particle reinforced Al matrix composites(Al MCCs) of 45 SiC_p/2024 and 55% SiC_p/A356 by ultrasonic brazing with ZnAlSi filler metal. Moreover , the microstructure and fracture appearance of the joints was investigated by SEM and EDS , and the shear strength of the joints was evaluated through shear test. The differences of the microstructures , the strength and fracture appearance of the Fe36Ni alloy and Al MCCs joints were analyzed in details. The results show that the filler metal and the base metal-sat both sides can form a good metallurgical bonding by ultrasonic brazing , and SiC particles are uniformly distributed in the brazed seam. The shear strength of Fe36Ni alloy with 45% SiC_p/2024Al joint are about 110-145 MPa , which is more than that of Fe36Ni alloy with 55% SiC_p/A356 joint of 75-85 MPa. The fracture occurs in the brazed seam of Fe36Ni alloy with 45% SiC_p/2024Al , while the joint of Fe36Ni alloy with the 55% SiC_p/A356 fractures on the interface of Fe36Ni and the filler metal.

Key words: Fe36Ni alloy; ultrasonic brazing; micro-structure; shear strength; fracture

Effect of adding micro amount rare earthelementLaNd on mechanical property of Bi5Sb8Sn solder alloy

LI Shuai , YAN Yanfu , FENG Lifang , ZHAO Yongmeng (College of Material Science and Engineering , Henan University of Science and Technology , Luoyang 471003 , China) . pp 9 - 12

Abstract: A new Bi5Sb8SnRE quaternary alloy was formed by adding different content of rare earthLa , Nd into Bi5Sb8Sn solder alloy to study the effect of its mechanical property and microstructure. The results shows that: The tensile strength and shear strength reaches a maximum are 58.30 MPa and 15.50 MPa , compared with Bi5Sb8Sn matrix , in which increased by 44.17% and 57.0% respectively when RE adds up to 0.2% . The Microscopic analysis shows that adding micro amount of RE could refine the microstructure. Meanwhile , more uniform microstructure , improvements of the mechanical properties were obtained with RE addition. However , the RE compounds are increased and the mechanical properties were decreased when the addition of RE more than 0.2wt. % .

Key words: Bi5Sb8SnRE quaternary alloy; La , Nd; tensile strength; shear strength

Inertia compensation of macro-micro robotic remote welding for pipeline repair in nuclear environment

GAO Sheng¹ , LI Haichao² , DU Aiguo² (1. College of Mechanical Science and Engineering , Northeast Petroleum University , Daqing 163318 , China; 2. State Key Laboratory of Advanced Welding and Joining , Harbin Institute of Technology , Harbin 150001 , China) . pp 13 - 16

Abstract: A teleoperated technology with the macro-micro-structure was proposed to perform the pipeline repair welding in the nuclear remote environment. A 6D force sensor was used to implement force control before pipeline assembly. Inertia compensation should be added to eliminate micro robot motion inertia influence. The inertia compensation algorithm and simulation experiments were studied and carried out. Simulation results show that the compensation algorithm can eliminate robot inertia force with the maximum force deviation not high than 2.5N and compensation torque deviation of 0.3Nm , which can meet the precision requirement of remote welding by macro-micro robot.

Key words: macro-micro robot; remote welding; force control; inertia compensation

Feature extraction for welding defect image based on contourlet transform and kernel principal component analysis

WU Yiquan^{1,2} , YE Zhilong¹ , WAN Hong¹ , GANG Tie² (1.